

REPORT DOCUMENTATION PAGE			Form Approved OMB NO. 0704-0188		
<p>The public reporting burden for this collection of information is estimated to average 1 hour per response, including the time for reviewing instructions, searching existing data sources, gathering and maintaining the data needed, and completing and reviewing the collection of information. Send comments regarding this burden estimate or any other aspect of this collection of information, including suggestions for reducing this burden, to Washington Headquarters Services, Directorate for Information Operations and Reports, 1215 Jefferson Davis Highway, Suite 1204, Arlington VA, 22202-4302. Respondents should be aware that notwithstanding any other provision of law, no person shall be subject to any penalty for failing to comply with a collection of information if it does not display a currently valid OMB control number.</p> <p>PLEASE DO NOT RETURN YOUR FORM TO THE ABOVE ADDRESS.</p>					
1. REPORT DATE (DD-MM-YYYY) 08-02-2012		2. REPORT TYPE Final Report		3. DATES COVERED (From - To) 1-Sep-2008 - 30-Nov-2010	
4. TITLE AND SUBTITLE AlInGa _N bandgap and doping engineering for visible laser diodes			5a. CONTRACT NUMBER W911NF-08-1-0378		
			5b. GRANT NUMBER		
			5c. PROGRAM ELEMENT NUMBER 8720T2		
6. AUTHORS Jingyu Lin, Hongxing Jiang			5d. PROJECT NUMBER		
			5e. TASK NUMBER		
			5f. WORK UNIT NUMBER		
7. PERFORMING ORGANIZATION NAMES AND ADDRESSES Texas Technical University Office of Research Services Texas Tech University Lubbock, TX 79409 -1035			8. PERFORMING ORGANIZATION REPORT NUMBER		
9. SPONSORING/MONITORING AGENCY NAME(S) AND ADDRESS(ES) U.S. Army Research Office P.O. Box 12211 Research Triangle Park, NC 27709-2211			10. SPONSOR/MONITOR'S ACRONYM(S) ARO		
			11. SPONSOR/MONITOR'S REPORT NUMBER(S) 55064-EL-DRP.7		
12. DISTRIBUTION AVAILABILITY STATEMENT Approved for Public Release; Distribution Unlimited					
13. SUPPLEMENTARY NOTES The views, opinions and/or findings contained in this report are those of the author(s) and should not be construed as an official Department of the Army position, policy or decision, unless so designated by other documentation.					
14. ABSTRACT There is a great need to develop chip-scale visible lasers for many applications, including laser sight, environmental monitoring, and compact pumping sources for ultra-short laser pulse generation, high luminous full color displays, new generation solid-state lighting, etc. The realization of chip-scale visible laser diodes (LDs) would provide significant benefits in terms of cost, volume, and the ability of photonic integration with other functional devices. Significant progress in nitride material technology has been achieved and high performance visible LEDs and near					
15. SUBJECT TERMS III-nitride semiconductors, visible lasers, photonics. p-type doping					
16. SECURITY CLASSIFICATION OF:			17. LIMITATION OF ABSTRACT UU	15. NUMBER OF PAGES	19a. NAME OF RESPONSIBLE PERSON Jingyu Lin
a. REPORT UU	b. ABSTRACT UU	c. THIS PAGE UU			19b. TELEPHONE NUMBER 806-742-3533

Report Title

AlInGa_N bandgap and doping engineering for visible laser diodes

ABSTRACT

There is a great need to develop chip-scale visible lasers for many applications, including laser sight, environmental monitoring, and compact pumping sources for ultra-short laser pulse generation, high luminous full color displays, new generation solid-state lighting, etc. The realization of chip-scale visible laser diodes (LDs) would provide significant benefits in terms of cost, volume, and the ability of photonic integration with other functional devices. Significant progress in nitride material technology has been achieved and high performance visible LEDs and near UV LDs based on InGa_N are now commercially available. However, many technological challenges remain to be overcome in order to realize InGa_N visible injection LDs. The two most outstanding issues are (i) high dislocation density which causes a premature device breakdown and (ii) low conductivity (or doping efficiency) of p-type Ga_N, which limits an efficient current injection. The objective of the proposed research is to develop improved growth and doping methods for achieving III-nitride materials with improved crystalline quality and conductivity and to aid in the development of III-nitride visible emitters operating at around 500 nm.

Enter List of papers submitted or published that acknowledge ARO support from the start of the project to the date of this printing. List the papers, including journal references, in the following categories:

(a) Papers published in peer-reviewed journals (N/A for none)

<u>Received</u>	<u>Paper</u>
-----------------	--------------

TOTAL:

Number of Papers published in peer-reviewed journals:

(b) Papers published in non-peer-reviewed journals (N/A for none)

<u>Received</u>	<u>Paper</u>
-----------------	--------------

TOTAL:

Number of Papers published in non peer-reviewed journals:

(c) Presentations

Number of Presentations: 0.00

Non Peer-Reviewed Conference Proceeding publications (other than abstracts):

<u>Received</u>	<u>Paper</u>
-----------------	--------------

TOTAL:

Number of Non Peer-Reviewed Conference Proceeding publications (other than abstracts):

Peer-Reviewed Conference Proceeding publications (other than abstracts):

<u>Received</u>	<u>Paper</u>
-----------------	--------------

TOTAL:

Number of Peer-Reviewed Conference Proceeding publications (other than abstracts):

(d) Manuscripts

Received Paper

TOTAL:

Number of Manuscripts:

Books

Received Paper

TOTAL:

Patents Submitted

Patents Awarded

Awards

Co-PI Professor Hongxing Jiang was elected a Fellow of the American Physical Society (APS) in 2010 for his seminal works in the area of III-nitride wide band-gap semiconductors.

Graduate Students

NAME	PERCENT SUPPORTED	Discipline
Bed Pantha	0.50	
Rajendra Dahal	0.50	
FTE Equivalent:	1.00	
Total Number:	2	

Names of Post Doctorates

NAME	PERCENT SUPPORTED
Jing Li	0.50
Hongmei Wang	0.50
FTE Equivalent:	1.00
Total Number:	2

Names of Faculty Supported

NAME	PERCENT SUPPORTED	National Academy Member
Jingyu Lin	0.08	
Hongxing Jiang	0.08	
FTE Equivalent:	0.16	
Total Number:	2	

Names of Under Graduate students supported

<u>NAME</u>	<u>PERCENT SUPPORTED</u>	Discipline
Matt Holman	0.10	Electrical Engineering
FTE Equivalent:	0.10	
Total Number:	1	

Student Metrics

This section only applies to graduating undergraduates supported by this agreement in this reporting period

The number of undergraduates funded by this agreement who graduated during this period:	1.00
The number of undergraduates funded by this agreement who graduated during this period with a degree in science, mathematics, engineering, or technology fields:.....	1.00
The number of undergraduates funded by your agreement who graduated during this period and will continue to pursue a graduate or Ph.D. degree in science, mathematics, engineering, or technology fields:.....	1.00
Number of graduating undergraduates who achieved a 3.5 GPA to 4.0 (4.0 max scale):.....	1.00
Number of graduating undergraduates funded by a DoD funded Center of Excellence grant for Education, Research and Engineering:.....	0.00
The number of undergraduates funded by your agreement who graduated during this period and intend to work for the Department of Defense	1.00
The number of undergraduates funded by your agreement who graduated during this period and will receive scholarships or fellowships for further studies in science, mathematics, engineering or technology fields:	0.00

Names of Personnel receiving masters degrees

<u>NAME</u>
Total Number:

Names of personnel receiving PHDs

<u>NAME</u>
Bed Pantha
Rajendra Dahal
Total Number:

Names of other research staff

<u>NAME</u>	<u>PERCENT SUPPORTED</u>
FTE Equivalent:	
Total Number:	

Sub Contractors (DD882)

Inventions (DD882)

Scientific Progress

see attached.

Technology Transfer

Final Report

Proposal No: 55064ELDRP
ARO Agreement No: W911NF-08-1-0378
Project Title: AlInGaN bandgap and doping engineering for visible laser diodes
PI Name: Jingyu Lin & Hongxing Jiang
PI Address: Nanophotonics Center, Texas Tech University,
Lubbock, TX 79409-3102
jingyu.lin@ttu.edu; hx.jiang@ttu.edu

Background

There is a great need to develop chip-scale visible lasers for many applications, including laser sight, environmental monitoring, and compact pumping sources for ultra-short laser pulse generation, high luminous full color displays, new generation solid-state lighting, etc. The realization of chip-scale visible laser diodes (LDs) would provide significant benefits in terms of cost, volume, and the ability of photonic integration with other functional devices.

Significant progress in nitride material technology has been achieved and high performance visible LEDs and near UV LDs based on InGaN are now commercially available. However, many technological challenges remain to be overcome in order to realize InGaN visible injection LDs. The two most outstanding issues are (i) high dislocation density which causes a premature device breakdown and (ii) low conductivity (or doping efficiency) of p-type GaN, which limits an efficient current injection. The objective of the proposed research is to develop improved growth and doping methods for achieving GaN and AlInGaN alloys with improved crystalline quality and conductivity and to aid in the development of III-nitride visible injection LDs operating at around 500 nm. Major accomplishments are summarized below:

1. Optimization of AlN epilayer templates

Our technical approaches include the use of high quality thick AlN template as a dislocation filter to reduce the parasitic conduction and trapping density in the device structure and to minimize the leakage current and premature breakdown.

As shown in Fig. 1, we have successfully transferred MOCVD processes for producing high quality AlN epilayer templates, which were developed in our home-built growth system, to production scale systems with 6 pieces of 2-inch wafer capability. We consider this a critical step, as this capability enables us to have an ample supply of templates to make multiple runs per day, which is necessary for the development of growth processes for green LD structures. Furthermore, we have significantly improved the crystalline quality of these AlN epi-templates, as evidenced by a decrease in the FWHM of the XRD rocking curve of the asymmetric (102) reflection peak from greater than 400 arcsec to below 300 arc.

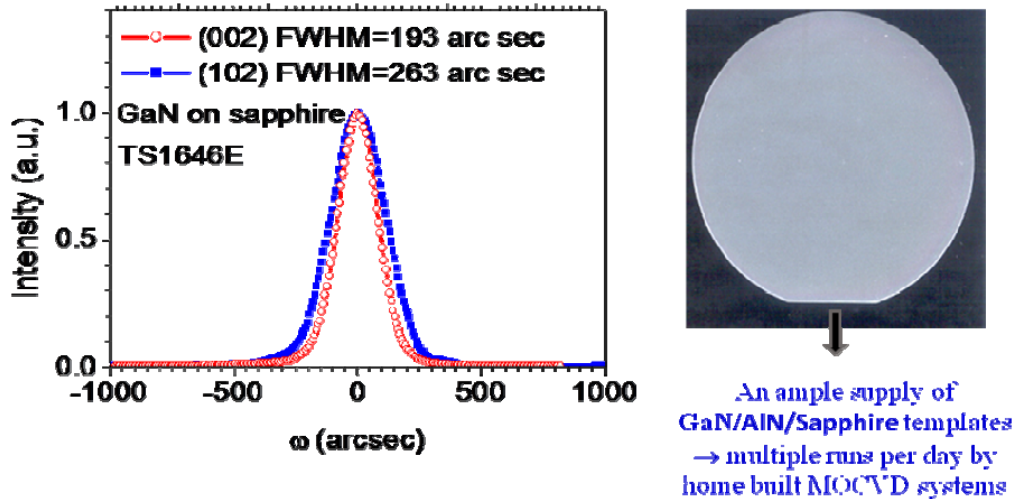


Figure 1: We have successfully transferred growth receipt of AlN epi-templates from home-built MOCVD system to production scale MOCVD system and improved the overall crystalline quality of AlN epi-templates.

2. Growth of single phase InGaN alloys

$\text{In}_x\text{Ga}_{1-x}\text{N}$, It has been exceedingly difficult to obtain homogeneous composition control and high quality InGaN materials in the middle indium composition range, $0.45 < x < 0.75$. There are only limited studies to address the MOCVD growth of the InGaN epilayer system in the entire composition range. Furthermore, detailed studies concerning the optical and transport properties of $\text{In}_x\text{Ga}_{1-x}\text{N}$ in the miscibility gap region ($0.45 < x < 0.75$) have not been possible due to the fact that these $\text{In}_x\text{Ga}_{1-x}\text{N}$ films generally are of very low crystalline quality and exhibit negligible PL emission. Our results in Fig. 2 have shown that by directly depositing on GaN or AlN epi-templates without buffer layers, InGaN epilayers of the entire alloy range without phase separation could be produced by MOCVD.

The attainment of single phase InGaN alloys inside the previously thought miscibility gap by MOCVD may be attributed to the following factors:

- the presence of biaxial strain between the InGaN thin film and the GaN or AlN epi-template,
- non-equilibrium growth processes taking place in epitaxial growth techniques like MOCVD,
- relatively low growth temperatures (The growth temperature varied from 730 to 610°C as the In-content was increased from 25% to 63%).

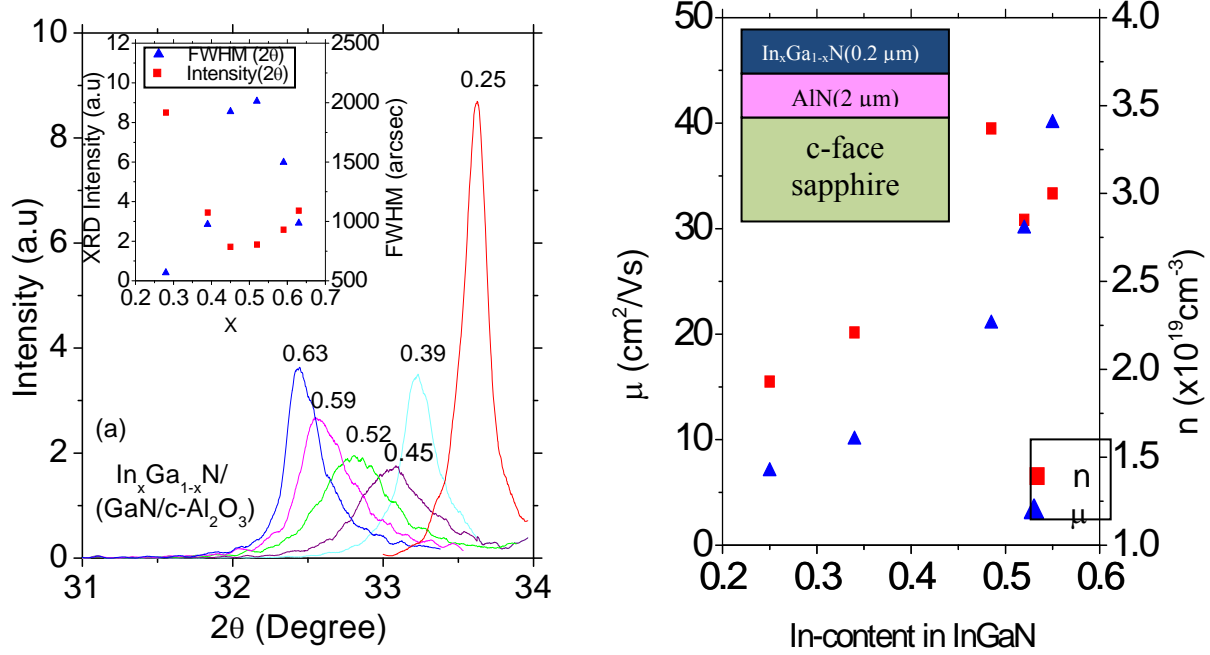


Figure 2: XRD spectra of θ - 2θ scans of (002) plane of $\text{In}_x\text{Ga}_{1-x}\text{N}$ grown on $\text{c-GaN/c-Al}_2\text{O}_3$ templates. The inset shows the XRD FWHM and relative intensity as functions of In-content. (b) Electron concentration and mobility of $\text{In}_x\text{Ga}_{1-x}\text{N}$ epilayers grown on $\text{c-AlN/Al}_2\text{O}_3$ templates as function of x . All curves, scanned down to InN peak position, have no multiple peaks, which implies that InGaN alloys are not phase separated. The reason for the increase in μ with increasing In-content could be the lower effective mass of the electrons. The measured 300 K electron mobility of $\text{In}_{0.55}\text{Ga}_{0.45}\text{N}$ alloys is about $40 \text{ cm}^2/\text{Vs}$ and of pure InN is as high as $1400 \text{ cm}^2/\text{Vs}$.

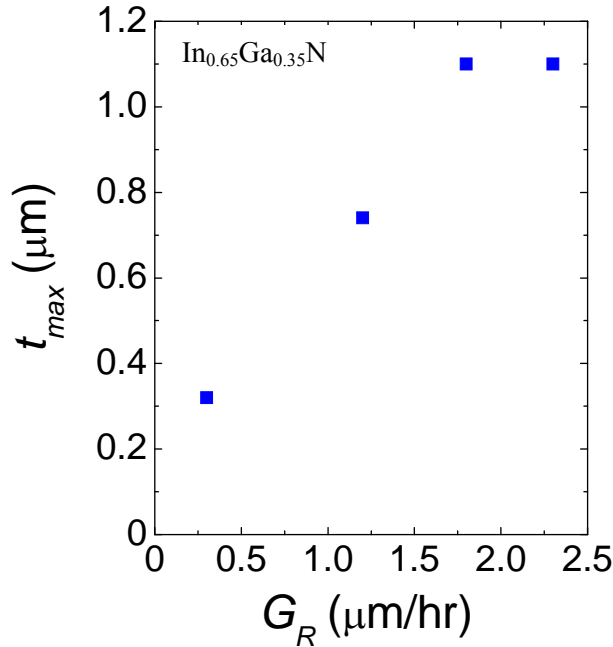


Figure 3: Maximum thickness t_{max} of $\text{In}_{0.65}\text{Ga}_{0.35}\text{N}$ that can be grown without phase separation, as a function of G_R . The bottom most spectrum is measured from a single phase 1 μm thick $\text{In}_{0.65}\text{Ga}_{0.35}\text{N}$ grown with $G_R = 1.8 \text{ μm/hr}$.

We have probed evolution of phase separation in $\text{In}_x\text{Ga}_{1-x}\text{N}$ alloys ($x \sim 0.65$) grown on AlN/sapphire templates by MOCVD. It was found that growth rate, G_R , is a key parameter and must be high enough ($>0.5 \mu\text{m/hr}$) in order to grow homogeneous and single phase InGaN alloys. Our results implied that conditions far from thermodynamic equilibrium are needed to suppress phase separation. Both structural and electrical properties were found to improve significantly with increasing G_R . The improvement in material quality is attributed to the suppression of phase separation with higher G_R . The maximum thickness of the single phase epilayer t_{max} (i.e. maximum thickness that can be grown without phase separation) was determined via *in-situ* interference pattern monitoring and found to be a function of G_R . As illustrated in Fig. 3, as G_R increases, t_{max} also increases. The maximum value of t_{max} for $\text{In}_{0.65}\text{Ga}_{0.35}\text{N}$ alloy was found to be $\sim 1.1 \mu\text{m}$ at $G_R > 1.8 \mu\text{m/hr}$.

3. Realization of p-type InGaN with relatively high In-contents

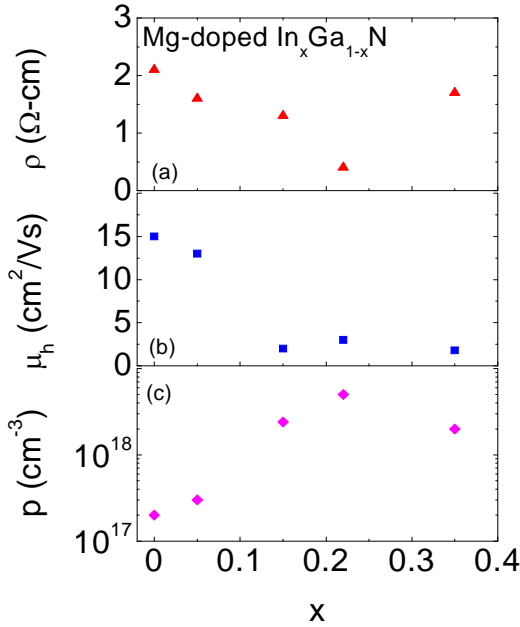


Figure 4: Room temperature (a) hole concentration p , (b) hole mobility μ_h , and (c) resistivity ρ as functions of In content (x) in Mg doped $\text{In}_x\text{Ga}_{1-x}\text{N}$ alloys. The data were determined by the Hall-effect measurement - the foremost established method to evaluate the carrier type and concentration as well as the energy levels of donors and acceptors in semiconductors.

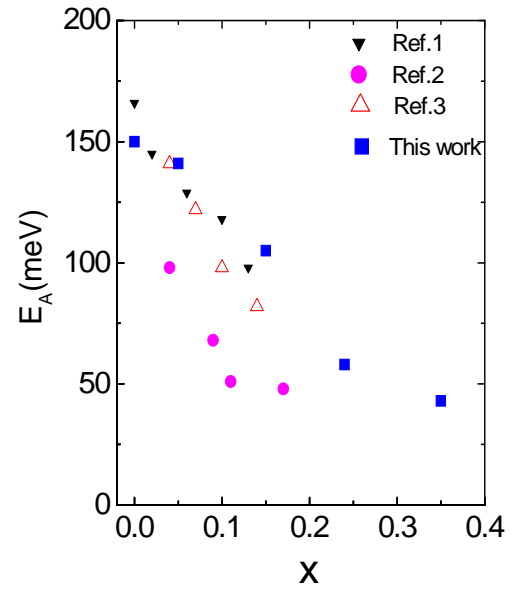


Figure 5: Energy level (E_A) of Mg acceptors in Mg doped p- $\text{In}_x\text{Ga}_{1-x}\text{N}$ alloys as a function of In content x . Data from references available up to $x = 0.17$ are also included [Ref. 1 - J. Appl. Phys. **93**, 3370 (2003); Ref. 2 - J. Cryst. Growth **221**, 267 (2000); Ref. 3 - Appl. Phys. Lett. **93**, 182108 (2008)].

Since the activation energies (E_A) of the Mg-acceptor decreases with a decrease in band gap energy, Mg-doped InGaN (InGaN:Mg) is expected to have a higher hole concentration (p) than Mg-doped GaN. Additionally, p-type InGaN is synthesized at a much lower temperature compared to p-type GaN. Thus, the use of p-type InGaN instead of p-type GaN in device structures is beneficial, particularly in devices such as green laser diodes and solar cells. We

have synthesized high In content p-InGaN by metal organic chemical vapor deposition (MOCVD). The room temperature electrical properties of p-type $\text{In}_x\text{Ga}_{1-x}\text{N}:\text{Mg}$ alloys as functions of x are plotted in Fig. 4. It was found that the hole concentration (p) continuously increases from 2×10^{17} for $x = 0$ (GaN) to $5 \times 10^{18} \text{cm}^{-3}$ when $x = 0.22$. μ_h was found to decrease from 15 to $1.8 \text{ cm}^2/\text{Vs}$ as x increases from 0 to 0.35. The variation in ρ with x shows that ρ decreases as x increases and reaches a minimum value of $0.4 \Omega \text{ cm}$ at $x = 0.22$ ($\text{In}_{0.22}\text{Ga}_{0.78}\text{N}$). This value of ρ is among the lowest reported for p-type InGaN.

As expected, the increase in free hole concentration in Mg-doped $\text{In}_x\text{Ga}_{1-x}\text{N}$ ($0 \leq x \leq 0.35$) alloys with increased In-content (x) is primarily due to the reduction in the activation energy (E_A) of Mg acceptors with x . The E_A values were obtained from the temperature dependence (Arrhenius plot) of free hole concentration. Figure 5 shows the plot of Mg acceptor activation energy (E_A) as a function of x along with other reported values for $\text{In}_x\text{Ga}_{1-x}\text{N}:\text{Mg}$ alloys. It was found that E_A continuously decreases with an increase in x . An E_A value as low as 43 meV was measured in $\text{In}_{0.35}\text{Ga}_{0.65}\text{N}:\text{Mg}$. This value is approximately four times smaller than that of Mg-doped GaN.

A typical Mg doping concentration around $5 \times 10^{19} \text{cm}^{-3}$ is needed in order to achieve p-type conduction in GaN with device applicable p-type conductivity ($\rho = 1 \Omega \text{ cm}$). In InGaN and particularly in high In-content InGaN, high Mg doping concentrations are required to compensate for high background electron concentration, which further reduced the measured values of E_A due to effects caused by high doping concentrations such as screening of the acceptor potential by free carriers. E_A of Mg as a function of In-content in Mg-doped InGaN shown in Fig. 2 was obtained from the optimized epilayers exhibiting the highest p-type conductivity. Note that E_A values of Mg in InGaN alloys measured by several groups are very consistent. Our values of E_A are the highest among the reported values for similar In-contents, which is related to the fact that the background electron concentration is the lowest in our InGaN materials.

$\text{In}_x\text{Ga}_{1-x}\text{N}$ materials with $x > 0.35$ were found to be generally highly n-type and conversion of these materials to p-type by Mg doping is still very difficult. Our results indicate that p-type conductivity in InGaN:Mg could be further improved if a better control of the background electron concentration could be achieved.

4. Understanding the origin of background electron concentration in $\text{In}_x\text{Ga}_{1-x}\text{N}$ alloys

The major obstacle for realizing p-type InGaN with relatively high In-contents is high background electron concentration (n). Since all InN and In-rich $\text{In}_x\text{Ga}_{1-x}\text{N}$ alloys grown by MOCVD possess high n ($\sim 10^{19} \text{cm}^{-3}$), it has been difficult to observe dependence on the growth or post-growth processing parameters and thus difficult to understand the cause of high n in InGaN.

Figure 6(a) shows the SIMS measurement results of $\text{In}_{0.24}\text{Ga}_{0.76}\text{N}$ alloys grown at two different V/III ratios (8,400 and 19,600). SIMS results show that concentrations of all investigated elements, H, O, Si, and C, are very high (on the order of 10^{19}cm^{-3} or even higher at a depth of $\sim 50 \text{ nm}$). The unusually high concentration of H and O near the surface could be due

to the post-growth surface contamination and artificial effects from SIMS measurements. Although H concentration in as-grown GaN can be as high as 10^{18} - 10^{19} cm $^{-3}$, the main donors in GaN have been attributed to Si and O. In the case of InN, both calculations and experiments indicated that H impurities, both interstitial (H_i) and substitutional (H_N), are the most probable candidates for high n and may be partially diffused out by post-growth thermal annealing.

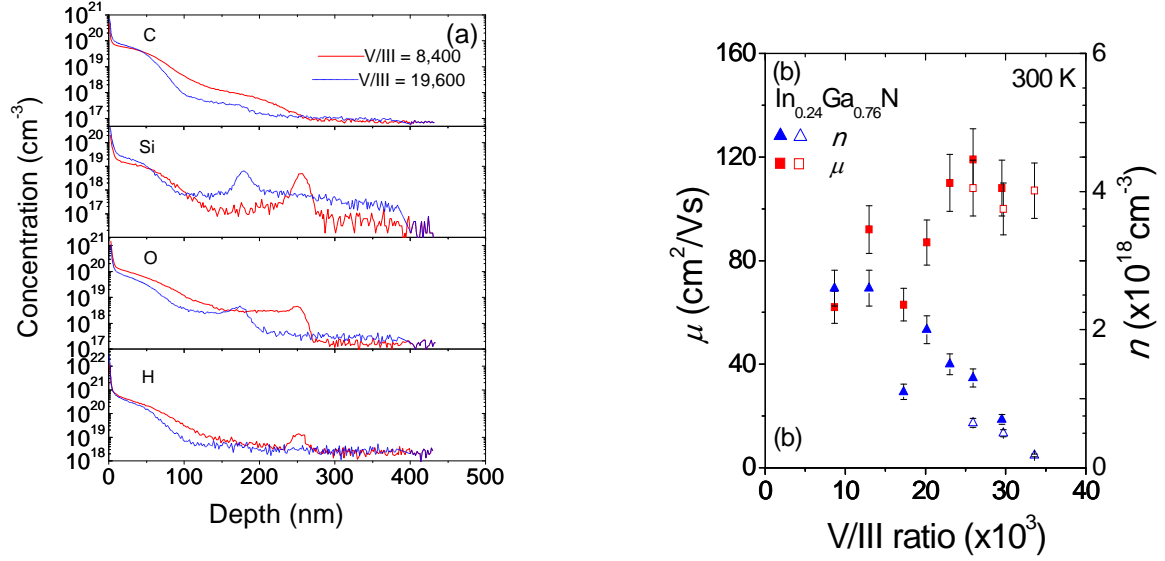
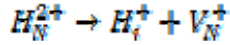


Figure 6: (a) SIMS profiles (H, O, Si, and C impurities) of In $_{0.24}$ Ga $_{0.76}$ N samples with two different V/III ratios of 8,400 and 19,600 (performed by Evan Analytical Group). (b) μ and n as functions of V/III ratio. Open (closed) symbol data are obtained by reducing (increasing) trimethylgallium and ammonia flow rate.

Since an increase in O or Si concentration with increasing x is not expected, they can be excluded as the dominant shallow donors in In $_x$ Ga $_{1-x}$ N alloys. Other possible shallow donor candidates include nitrogen vacancies (V_N). The contribution of V_N to the background electron concentration in GaN is expected to be low due to the high formation energy of V_N in GaN. However, nitrogen vacancies are the most probable cause of a residue electron concentration on the order of 10^{17} cm $^{-3}$ in a typical good quality, unintentionally doped GaN, due to the deficiency of N atoms during MOCVD growth. In contrast, the deficiency of N atom is much more severe in InGaN alloys than in GaN due to lower cracking efficiency of NH $_3$ at reduced growth temperatures (the growth temperature decreases from 1050 °C for GaN to \sim 600 °C for In-rich InGaN alloys). This N deficiency significantly increases the concentration of V_N .

To understand the severity of nitrogen deficiencies, we have monitored n for In $_{0.24}$ Ga $_{0.76}$ N alloys grown with varying V/III ratios and found that the values of n decrease with increasing V/III ratio, as shown in Fig. 6 (b). A higher V/III ratio should provide more active nitrogen atoms during growth and compensate for the deficiency of N atoms, which in turn reduces the concentration of V_N and/or H_N . The overall material quality also improved with increasing V/III ratio as evidenced by a linear increase in electron mobility with an increase in the V/III ratio. These results seem to suggest that in addition to interstitial H_i , V_N and/or H_N are also major donors in InGaN, particularly in In-rich InGaN alloys.

It has been shown that the background electron concentration can be reduced via out diffusion of H by thermal annealing. However, n values in such annealed samples remain very high, implying the possibility of other donors. Our results suggest that singly charged V_N related impurities are one of the major causes of residual n in InGaN. In such a context, the main donors in InN or In-rich InGaN alloys are H and V_N related impurities. In addition to interstitial H_i^+ , substitution H_N^{2+} is also a potential cause of high n in InN. H_N^{2+} can migrate via the following dissociation process:



If we assume concentrations of H_N^{2+} , H_i^+ , and V_N^+ in an as-grown InN or In-rich InGaN are the same, from the above reaction, we have $N[H_N^{2+}] = N[H_i^+] = N[V_N^+]$, while annealing can only reduce n by half via out-diffusion of H_i^+ (*in-situ* incorporated H_i^+ and H_i^+ formed by dissociation process of H_N^{2+} during annealing). V_N^+ cannot be diffused out and is thus responsible for residual background electron concentration in annealed materials.

5. LD device design, fabrication, and characterization

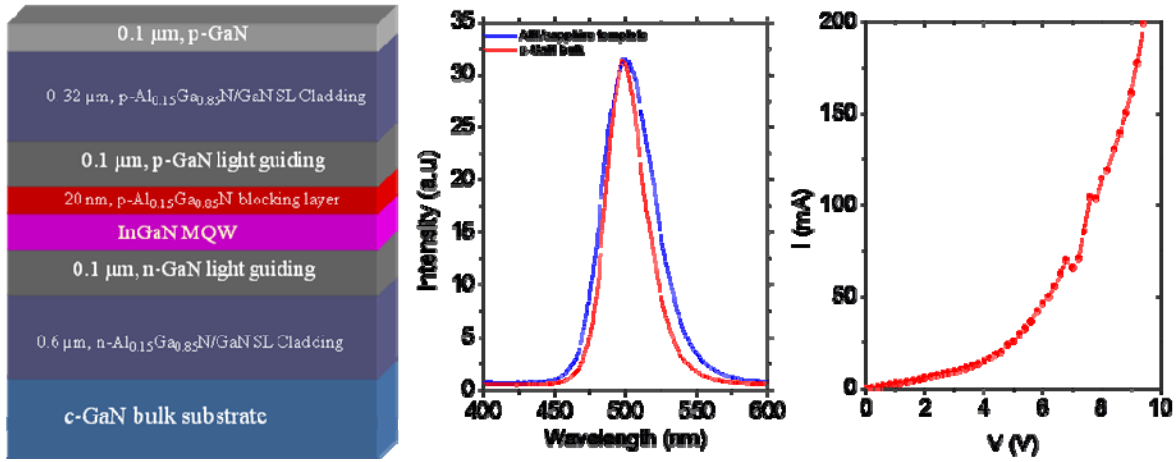


Figure 7: (Left) LD structure grown on c-plane GaN bulk substrate; (Middle) EL spectra of LDs grown on AlN/sapphire template vs. on c-bulk GaN; (Right) I-V characteristics of LD on c-GaN bulk.

- We have successfully evolved our green light emitting diode (LED) structure to 500 nm LD structure by inserting cladding and light guiding layers. We have obtained a significant improvement in optical emission efficiency by depositing the emitter structures on AlN templates.
- We have also carried out preliminary studies of MOCVD growth of GaN epilayers and LD structures on bulk GaN substrates synthesized by HVPE. Compared to LD structures grown on AlN/sapphire templates, LD structures grown on GaN bulk substrates exhibit lower

dislocation density (narrower XRD and EL emission spectra linewidth) and comparable output optical power [Fig. 7].

- Ridge waveguides with 5 to 20 μm widths and 500 to 1500 μm lengths were fabricated. We have also developed a method for preparing the laser cavity by controlled mechanical polishing. The polished laser facets has a root-mean-square surface roughness of ~ 0.5 nm over a 10 μm x 10 μm scanning area as probed by AFM [Fig. 8].

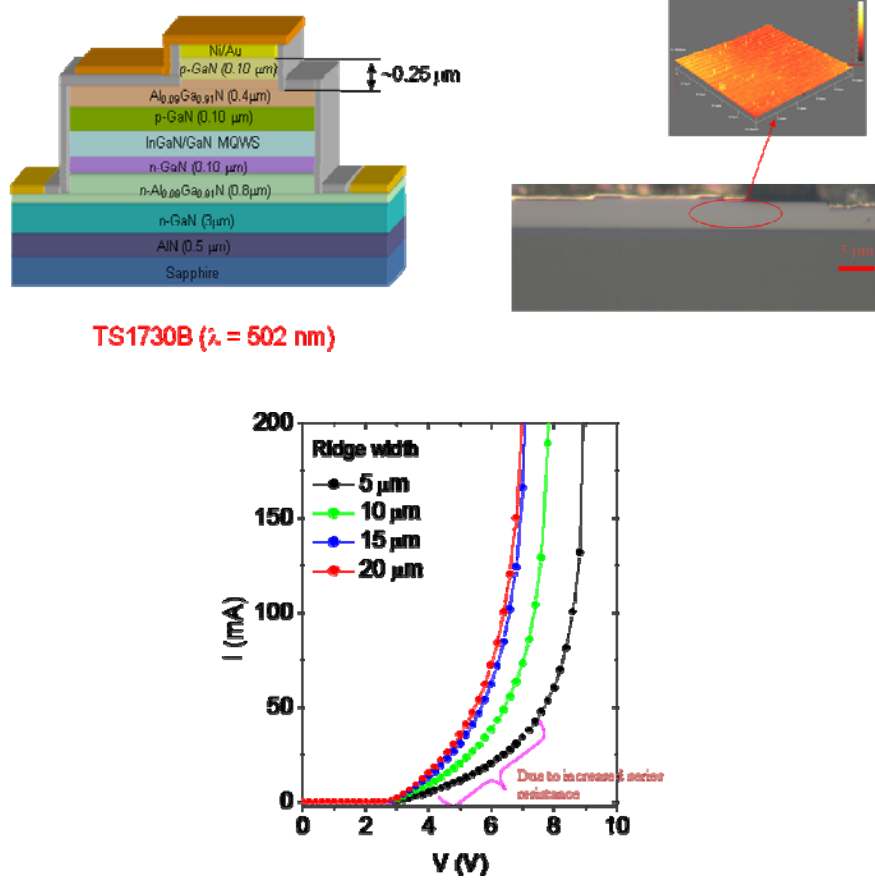
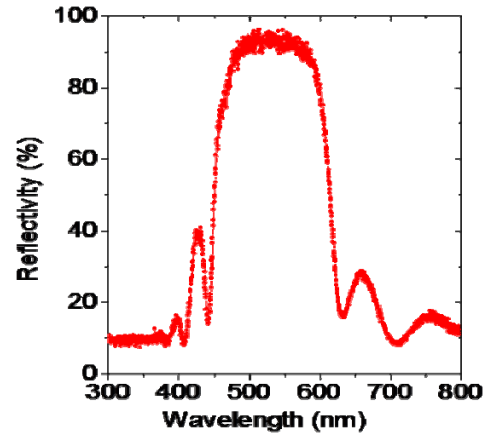
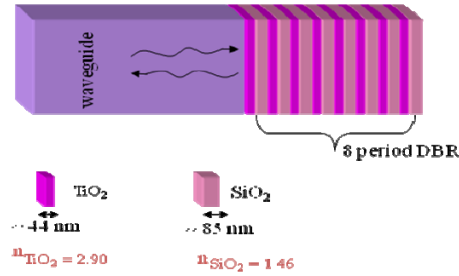


Figure 8: (Left) Schematic diagram of fabricated ridge waveguide laser. (Right) Optical microscopy image of cross-section of ridge waveguide laser. The laser facets were prepared by slow and controlled polishing. AFM scan over polished surface of 10 mm x 10 mm area showed rms ~ 0.5 nm. (Bottom) I-V characteristics of fabricated LEDs, indicating that the operating voltage increases with decreasing ridge width and further improvement in device processing is necessary.

- We are also developing the processes for obtaining $\frac{1}{4}$ wave reflectors for 500 nm operation based on $\text{SiO}_2/\text{TiO}_2$ multi-layers for the laser cavity to minimize the optical loss [Fig. 9].

TiO₂ and SiO₂ multilayers were deposited by e-beam evaporator and thickness of each layer has been optimized. The eight pair DBR exhibits a reflectivity ~ 95% at around 500 nm.



The physical parameters are

$$t_{\text{SiO}_2} = \frac{\lambda_0}{4n_{\text{SiO}_2}} = 85 \text{ nm}$$

$$t_{\text{TiO}_2} = \frac{\lambda_0}{4n_{\text{TiO}_2}} = 44 \text{ nm} \quad \text{for } \lambda_0 = 500 \text{ nm}$$

Figure 9: Highly reflective TiO₂/SiO₂ dielectric multilayer coating for green laser has been developed.

Publications

- Z. Y. Fan, J. Y. Lin, and H. X. Jiang, "III-nitride micro-emitter arrays: development and applications," Special Issue, J. Phys. D: Appl. Phys. **41**, 094001 (2008); invited; [doi:10.1088/0022-3727/41/9/094001](https://doi.org/10.1088/0022-3727/41/9/094001).
- R. Dahal, B. Pantha, J. Li, J. Y. Lin, and H. X. Jiang, "InGaN/GaN multiple quantum well solar cells with long operating wavelengths," Appl. Phys. Lett. **94**, 063505 (2009); [doi:10.1063/1.3081123](https://doi.org/10.1063/1.3081123).
- B. N. Pantha, A. Sedhain, J. Li, J. Y. Lin, and H. X. Jiang, "Electrical and optical properties of p-type InGaN," Appl. Phys. Lett. **95**, 261904 (2009); [doi:10.1063/1.3279149](https://doi.org/10.1063/1.3279149).
- B. N. Pantha, A. Sedhain, J. Li, J. Y. Lin, and H. X. Jiang, "Achieving p-In_xGa_{1-x}N alloys with high In contents," Proc. SPIE 7602, 76020Z (2010); [doi:10.1117/12.842313](https://doi.org/10.1117/12.842313).
- B. N. Pantha, J. Y. Lin, and H. X. Jiang, "III-nitride nanostructures for energy generation," Proc. SPIE 7608, 76081I (2010); invited; [doi:10.1117/12.840726](https://doi.org/10.1117/12.840726).

Principal investigators and their group were relocated from Kansas State University to Texas Tech University during the project period. They currently hold the inaugural Edward E. Whitacre, Jr. Endowed Chair and Linda F. Whitacre Endowed Chair at Texas Tech University (Mr. Whitacre is the former CEO of AT & T). During the supporting period, the Co-PI, Prof. Hongxing Jiang, was also elected as the American Physical Society fellow. Dr Jiang was nominated for "his seminal works in the area of III-nitride wide bandgap semiconductors. In particular, for his significant contributions to the understanding of fundamental optical and defect properties and practical applications of III-nitrides and pioneering contributions to the field of nanophotonics."